Brain
Pathology

Region-specific preservation of Purkinje cell morphology and motor behavior in the ATXN1[82Q] mouse model of spinocerebellar ataxia 1

Joshua J. White[1] 🔘 | Laurens W. J. Bosman[1] 🔘 | Francois G. C. Blot[1] 🔘 |
Catarina Osório[1] 🔘 | Bram W. Kuppens[1] | Wilhelmina H. J. J. Krijnen[1] |
Charlotte Andriessen[1] | Chris I. De Zeeuw[1,2] 🔘 | Dick Jaarsma[1] 🔘 | Martijn Schonewille[1] 🔘

[1]Department of Neuroscience, Erasmus MC, Rotterdam, Netherlands

[2]Netherlands Institute for Neuroscience, Royal Academy of Arts and Sciences, Amsterdam, Netherlands

Correspondence
Martijn Schonewille, Dick Jaarsma, and Chris I. De Zeeuw, Department of Neuroscience, Erasmus Medical Center, Rotterdam 3015 AA, Netherlands
Email: m.schonewille@erasmusmc.nl (M. S.), d.jaarsma@erasmusmc.nl (D. J.), c.dezeeuw@erasmusmc.nl (C. I. D. Z.)

Funding information
Albinism NIN-Friend Foundation; Nederlandse Organisatie voor Wetenschappelijk Onderzoek, Grant/Award Number: ALW, INTENSE NWO-LSH and VENI; ZonMw, Grant/Award Number: Off-road Fellowship and memorabel (733050810); H2020 European Research Council, Grant/Award Number: ERC-Adv, ERC-PoC and Stg #680235; EU-Listen; Medical NeuroDelta

Abstract

Purkinje cells are the primary processing units of the cerebellar cortex and display molecular heterogeneity that aligns with differences in physiological properties, projection patterns, and susceptibility to disease. In particular, multiple mouse models that feature Purkinje cell degeneration are characterized by incomplete and patterned Purkinje cell degeneration, suggestive of relative sparing of Purkinje cell subpopulations, such as those expressing Aldolase C/zebrinII (AldoC) or residing in the vestibulo-cerebellum. Here, we investigated a well-characterized Purkinje cell-specific mouse model for spinocerebellar ataxia type 1 (SCA1) that expresses human ATXN1 with a polyQ expansion (82Q). Our pathological analysis confirms previous findings that Purkinje cells of the vestibulo-cerebellum, i.e., the flocculonodular lobes, and crus I are relatively spared from key pathological hallmarks: somatodendritic atrophy, and the appearance of p62/SQSTM1-positive inclusions. However, immunohistological analysis of transgene expression revealed that spared Purkinje cells do not express mutant ATXN1 protein, indicating the sparing of Purkinje cells can be explained by an absence of transgene expression. Additionally, we found that Purkinje cells in other cerebellar lobules that typically express AldoC, not only display severe pathology but also show loss of AldoC expression. The relatively preserved flocculonodular lobes and crus I showed a substantial fraction of Purkinje cells that expressed the mutant protein and displayed pathology as well as loss of AldoC expression. Despite considerable pathology in these lobules, behavioral analyses demonstrated a relative sparing of related functions, suggestive of sufficient functional cerebellar reserve. Together, the data indicate that mutant ATXN1 affects both AldoC-positive and AldoC-negative Purkinje cells and disrupts normal parasagittal AldoC expression in Purkinje

Joshua J. White and Laurens W. J. Bosman contributed equally to this work.

cells. Our results show that, in a mouse model otherwise characterized by widespread Purkinje cell degeneration, sparing of specific subpopulations is sufficient to maintain normal performance of specific behaviors within the context of the functional, modular map of the cerebellum.

KEYWORDS
motor learning, spinocerebellar ataxia, patterned neurodegeneration

1 | INTRODUCTION

Neurodegenerative diseases, whether sporadic or genetic, typically follow a specific pattern of neural death or degeneration/atrophy affecting one or a few specific cell types even when the genetic defect is expressed throughout the brain (1,2). The impact on a specific cell type or brain region is likely related to gene expression patterns, environmental factors, and neurophysiological activity and leads to the specific set of symptoms that characterize a neurological or psychiatric disease. In genetic disorders, for a specific cell type to be directly affected by a mutation requires that the cell expresses the mutated gene and depends on the interaction of the gene with the general homeostasis and physiology of the cell. Similarly, single mutations are able to affect only a subset of a particular neuronal cell type, provided that there is sufficient differentiation within that type of neuron. Along these lines, molecular markers have been identified for selective populations of vulnerable or non-vulnerable motor neurons in amyotrophic lateral sclerosis (3,4), pyramidal neurons in dementia (5), and dopaminergic neurons in Parkinson's Disorder (6,7).

Cerebellar ataxias form a large group of neurodegenerative diseases, with well over 100 genetic and sporadic forms (8–10). In many of these, dysfunction or degeneration of cerebellar Purkinje cells is a major cause of the clinical symptoms (9,11–14). Despite this common disease target, individual forms of cerebellar ataxia show differences in the symptomatic progress of the disease (15). Possibly, these differences are at least in part explained by differential vulnerability of Purkinje cells, as has been demonstrated in mouse models (16). These mouse models represent a unique substrate to investigate factors underlying differential vulnerability of neurons because Purkinje cells are implicated in multiple neurodegenerative disorders in which they are predominantly affected even when genetic mutations are expressed throughout the brain (9,17).

Purkinje cells can be divided into groups on the basis of differential gene expression and activity patterns (18–20). The highly ordered architecture of the cerebellar cortex, and modular organization of Purkinje cells enables precise behavioral, physiological, and neuropathological investigation of Purkinje cells subpopulations (21). The expression of Aldolase C (AldoC also known as Zebrin II (22,23)) and other markers (24) map onto the cerebellar cortex in such a way that they form parasagittal stripes that are either predominantly AldoC negative or positive (19,25,26). Behaviors mediated by the cerebellum have been linked to regions that are either AldoC positive or negative (27). These regional specifications mean that lesions or degeneration within specific areas of the cerebellum would likely result in specific behavioral deficits even though redundancy of the cerebellar circuitry assures that behavior can be maintained if the lesion does not affect the entire region (28–30).

Consequently, studies on patterned degeneration in mouse models of Purkinje cell degeneration/atrophy have focused on the relationship with the expression of AldoC (16). In healthy animals, AldoC-negative Purkinje cells have a higher intrinsic firing rate (20,31,32), which may lead to susceptibility itself because of increased likelihood of excitotoxicity (4,33). Under pathological conditions, the situation may be more complicated as, for instance, in a mouse model for spinocerebellar ataxia type 1 (SCA1), the overall firing rates of Purkinje cells proved to be reduced (34), but this appears to follow initial Purkinje cell atrophy.

Because the mechanism of differential Purkinje cell degeneration is not well understood, we have analyzed morphological and behavioral phenotypes in ATXN1[82Q] mice, a mouse model for SCA1. ATXN1[82Q] mice express copies of a polyQ-expanded *ATXN1* gene in a Purkinje cell-specific manner, which leads to obvious Purkinje cell atrophy beginning at 3 and 4 weeks (35) and locomotor deficits at 5 and 6 weeks (36). Previous studies have indicated regional variations in the degeneration of Purkinje cells in ATXN1[82Q] mice, particularly sparing the vestibulo-cerebellum (flocculonodular lobes) (36,37). Because these regions are known to be predominantly AldoC positive, we aimed to more systematically investigate this mouse model for a link between Purkinje cell vulnerability and AldoC expression, and to determine the extent to which differential vulnerability impacts cerebellum-dependent behaviors. However, we found that instead of correlating with AldoC, selective sparing of the flocculonodular lobe, and also crus I, correlated with no or minimal transgene expression. To examine the functional impact of the region-specific sparing of a subset of Purkinje cells, we tested behaviors related to these regions and found that, unlike the clear and progressive

locomotor impairment in ATXN1[82Q] mice, the behaviors related to surviving regions are indeed preserved.

2 | METHODS

2.1 | Mice

All experiments were performed on heterozygous transgenic mice of both sexes expressing *ATXN1* with an expanded CAG repeat and their wild-type littermates. The mutant mice overexpress human *ATXN1* cDNA containing an 82 CAG repeat under the Purkinje cell-specific L7/Pcp2 promoter (Tg(Pcp2-ATXN1*82Q)5Horr). The generation of this mouse line has been described as strain "B05" in (35). The mice were kept on an FVB/NHsd background, except for those involved in compensatory eye-movement experiments. For the latter, F1 offspring from crossings between FVB/NHsd and C57Bl6/J mice were used. The mice were kindly provided by Dr. Harry T. Orr at the University of Minnesota, Minneapolis, MN, USA. Mice were group housed with a 12 h light/dark cycle and had free access to standard laboratory food and water. All experiments were performed according to institutional guidelines as overseen by the Animal Welfare Board of the Erasmus MC, following Dutch and EU legislation. Prior to the start of the experiments, a project license for the animal experiments performed for this study was obtained from the Dutch national authority and filed under no. AVD101002015273.

2.2 | Histology

Mice of 6, 12, 18, and 24 weeks old (±3 days) were included in the experiments. Mice were deeply anesthetized with pentobarbital (80 mg/kg administered intraperitoneally) and perfused with saline and 4% paraformaldehyde in series. Tissue was then post-fixed in 4% paraformaldehyde for 1 and 2 h before being placed in 10% sucrose in phosphate buffer overnight at 4°C. The following day, brains were embedded in gelatin (FujiFilm Wako, #077-03155). They were then placed in a solution of 30% sucrose and 4% paraformaldehyde for 1 and 2 h before being placed in a solution of only 30% sucrose overnight at 4°C. The following day the embedded brains were sectioned at 40 μm on a freezing microtome and placed free-floating into wells of phosphate-buffered saline (PBS). Brain sections were then incubated with primary antibodies in a solution of 4% normal horse serum, 0.2% Triton (Sigma-Aldrich, #X100), and PBS overnight at room temperature or 2 nights at 4°C. Sections were then washed in PBS 3-5x for 5–10 min and then incubated for 2 h in secondary antibodies in 4% Normal Horse Serum, 0.2% Triton, and PBS at room temperature. For light microscopy sections, staining was visualized with DAB solution in H_2O_2 and dried on the slide overnight before being counter-stained with thionin, dehydrated, and cover-slipped. For fluorescence microscopy, sections were incubated in DAPI solution (Thermo Fisher Scientific, Cat# D3571, RRID:AB_2307445) for 10 min then washed and mounted on coverslips, dried for 30 min at 37°C, and then mounted onto slides with Mowiol (Calbiochem, La Jolla, CA, USA). Light microscopy images were acquired with a NanoZoomer (Hamamatsu). Fluorescent images were acquired with an LSM700 confocal (Zeiss) or Axio Imager.M2 (Zeiss). Images were adjusted for contrast and brightness in Adobe Photoshop. Primary antibodies: calbindin (Calbindin D-28 K, 1:10000, mouse, Swant 300), AldoC (aldolase C, 1:1000, goat, SC-12065), p62 (SQSTM1/P62 Abcam: 56416, mouse, 1:1000), and Ataxin-1 11750 (gift from Dr. Huda Zoghbi, rabbit, 1:1000). Secondary antibodies: Cy3 (1:500, donkey anti-rabbit, Jackson), Alexa-488 (1:500, donkey anti-goat, Jackson), HRP anti-mouse (1:500, Dako P0260), and NeuroTrace 435 (Invitrogen). For examination of the percentage of Purkinje cells expressing mutant protein, select lobules from three sections each from three ATXN1[82Q] mice were counted.

2.3 | Behavioral assays – locomotion

Locomotor patterns were studied using the fully automated ErasmusLadder (Noldus, Wageningen, The Netherlands), consisting of a horizontal ladder counting 37 rungs on each side in between two shelter boxes as described previously (38). Mice were acclimated to the ErasmusLadder for 20 min. the first day and then given 2 days of rest. Next, mice were tested with one session a day for 5 days at age 6 weeks, then with one weekly session until 24 weeks. At the start of each session, the mouse was placed in one of the two shelter boxes. After a period varying from 9 to 11 s, a LED light turned on in the shelter box signaling that the mouse was supposed to leave the box. If the mouse left the box before the light turned on, a strong air flow drove the mouse back into the box, and the waiting period restarted. If the mouse did not leave the box within 3 s after the light turned on, a strong air flow drove the mouse out of the box. When the mouse arrived in the other box, the lights and air flow were turned off and the waiting period from 9 to 11 s started again, after which the mouse was supposed to start the next trial, etc. A session consisted of 42 consecutive crossings of the ladder with 8–12 s of rest in between trials. The sequence of consecutive mice participating in a session was identical for every experiment and inter-experimental variation of the environment was kept at a minimum. All sessions were "non-perturbed sessions" (38) implying that no obstacle rungs were elevated during the trials.

The relative fraction of different step types and step times was calculated to analyze locomotor patterns.

Step time was defined as the time that elapsed between the onsets of two consecutive touches. Step types were defined based on the step direction, the distance between two consecutive touches (step length), and whether an upper or lower rung was touched. All steps that are not in the walking direction were defined as back steps. All forward steps that terminated on an upper rung were sorted to three distinct categories according to step length: short steps (one or two rungs further), long steps (three or four rungs further), and jumps (five or more rungs further). All forward steps that terminated on a lower rung were sorted in lower short steps, lower long steps, and lower jumps as is described for the upper rung steps. The number of each step type is quantified as a percentage of the total amount of steps per trial.

Mice were also evaluated on a 1-meter-long and 12-mm-diameter balance beam at ages 7, 12, 18, and 24 weeks. One end of the beam was supported by a metal pole and the other end terminated in a home cage, with the beam suspending horizontally 50 cm above the surface. Usual parameters are the crossing time and the number of slips per run (39). However, the latter parameter is inadequate for the assessment of the severe ATXN1[82Q] phenotype. Hence, this is replaced by the percentage of runs where the end of the beam is reached (percentage of successful trials).

2.4 | Behavioral assays – licking

The rhythmicity of spontaneous licking was derived from measurements of the junction potential between an aluminum floor plate and the spout of a normal drinking bottle in a normal home cage with the use of an AD converter operating at a sample rate of 6 kHz (RZ2, Tucker-Davis Technologies, Alachua, FL, USA) as described before (40). Mice were water deprived for 2 h prior to the start of the recording and subsequently measured overnight (>12 h) at the ages of 7, 12, 18, and 24 weeks. The data from the first hour were disregarded, as the mice typically showed irregular, explorative behavior during this period. A lick was recognized in the junction potential recording as a stereotypic event and detected by threshold crossing using SpikeTrain (Neurasmus BV, Rotterdam, The Netherlands). All traces were inspected visually and incorrectly detected events were corrected. We restricted our analysis to bouts of rhythmic licking, which were defined by the occurrence of at least two licks with a maximal inter-lick interval (ILI) of 150 ms and minimum of 50 ms. The upper and lower cut-offs were established based on histograms of ILIs measured in past and present recordings. The ILIs were defined using cut-offs well over 150 ms and the graphs demonstrate a bell-shaped curve between 50 and 150 ms which encompasses ± 90% of all ILIs, while ILIs with

lengths beyond 150 ms show no such organization. Prior to analysis, the total amount of licks was counted for each genotype to confirm an equal magnitude of data. The average licking rate, median number of licks per licking bout, and coefficient of variance (CV2) of subsequent ILIs within licking bouts were calculated for each mouse and averaged per genotype. The CV2

was calculated as $2 \times \sqrt{\frac{|ILI_{n+1} - ILI_n|^2}{(ILI_{n+1} + ILI_n)}}$ (41).

2.5 | Behavioral assays – compensatory eye movements

Compensatory eye movements were tracked in head-fixed mice implanted with a custom-built pedestal. For surgery, mice were anesthetized with isoflurane, body temperature was maintained at 37°C, and ophthalmic ointment (Duratears, Alcon®) was applied to prevent the eyes from desiccating. The scalp, after shaving and treatment with Xylocaine (AstraZenica), was opened to expose the skull. The periosteum was scraped away, again after treatment with Xylocaine, and the bone was covered with Optibond (Kerr). The pedestal was attached to the skull with Charisma (Heraeus Kulzer). Both Optibond and Charisma are cured with UV light. As anti-inflammatory agent and analgesic, carpofen (0.5 mg/ml, Rimadyl Cattle) and bupivacaine (0.1 mg/ml, Actavis) were used, respectively. The surgery was performed at least 2 days prior to the start of the experiment. For eye movement testing, mice were first head fixed in the center of a turntable (Ø 60 cm), surrounded by a paper drum with random-dotted pattern (Ø 63 cm, dot size 2°) and tested for baseline optokinetic (OKR), vestibulo-ocular (VOR), and visual vestibulo-ocular (VVOR) responses. To this end, we subjected mice to 10° peak-to-peak sinusoidal rotations at 0.1–1.0 Hz of the visual stimulus (OKR), the table in the dark (VOR), or the table in the light (VVOR). The following day the ability for adaptation was tested using 6 × 5 min training sessions during which the visual stimulus rotated out of phase with the table in light, aiming to increase the gain of the VOR, with a VOR probe performed in darkness at the start and after every 5 min of training. Data were acquired with a CCD camera and video acquisition software (ISCAN Inc.) which tracked the movements of the pupil in relation to the corneal reflection created by infrared lamps. A calibration was performed at the beginning and end of each measurement. The calibration is required to turn the pixels of the video into angles when analyzing the acquired data. To determine the gain (size) and phase (timing), the eye movement and stimulus traces were differentiated to velocity signals, averaged across cycles and fitted with a sine; the amplitude of the fitted eye movement divided by stimulus was taken as the gain and the shift in time was taken as phase (in degrees of the cycle).

3 | RESULTS

3.1 | Purkinje cell degeneration in the ATXN1[82Q] mouse is regionally specific

The ATXN1[82Q] mouse (line B05) is a transgenic line that overexpresses human ATXN1 with an 82 CAG repeat under control of the Purkinje cell-specific L7/Pcp2 promoter (35). ATXN1[82Q] mice develop progressive degeneration of Purkinje cells, predominantly consisting of gradual somatodendritic atrophy starting from 4 to 6 weeks and ultimately culminating in late-onset Purkinje cell death after 6–8 months of age (36). Following up on previous reports that a subset of Purkinje cells are spared from pathology (36), particularly those residing in the flocculonodular lobes, we first mapped the spatiotemporal distribution of Purkinje cell somatodendritic atrophy in sagittal and coronal sections stained for calbindin, a Purkinje cell-specific marker in the cerebellum. Widespread somatodendritic atrophy is clearly visible in the majority of Purkinje cells in sagittal sections at 12 weeks (Figure 1). The nodulus (lobule X), especially its ventral side, the flocculus including the ventral paraflocculus, and crus I instead are relatively spared (Figure 1D and Figure 1K,L). Notably, other lobules showed a few sporadic examples where Purkinje cells are spared. The same picture emerged from a more systematic analysis of coronal series from ATXN1[82Q] mice from 6 to 24 weeks of age (Figure 2). At 6 weeks of age, only mild Purkinje cell atrophy is manifested in the form of non-uniform expression of calbindin in the molecular layer of the cerebellar cortex (Figure 2A,C,E,G). Purkinje cell atrophy then progressed steadily from 12 to 18 and 24 weeks. However, the spared areas of the cerebellar cortex are spared at all ages. For instance, the flocculus still exhibits normal Purkinje cell calbindin expression and morphology at 24 weeks when the anterior vermis exhibits severe Purkinje cell atrophy (Figure 2).

3.2 | AldoC expression is disrupted in ATXN1[82Q] mice

Having established the spatial distribution of Purkinje cell somatodendritic atrophy, we next investigated the relationship of Purkinje cell atrophy and AldoC (Figure 3). Surprisingly, we found that AldoC expression was dramatically altered in ATXN1[82Q] mice at all ages investigated: many regions known to express AldoC in wild-type mice either do not express AldoC or the expression is patchy (Figure 3A-D). Closer analysis showed that AldoC expression was only spared in Purkinje cells that did not show somatodendritic atrophy. Thus, AldoC expression is largely normal in the flocculonodular lobes and crus I. To a lesser extent, AldoC was also still expressed in lobule VI, although more patchy than is typical in wild-type mice (Figure 3C,D). Instead, AldoC expression was mostly absent in the rest of the central and posterior cerebellum, which typically expresses large AldoC-positive bands (42). In the anterior vermis characterized by three thin stripes of AldoC-positive Purkinje cells (25), these stripes are unreliably present in ATXN1[82Q] mice.
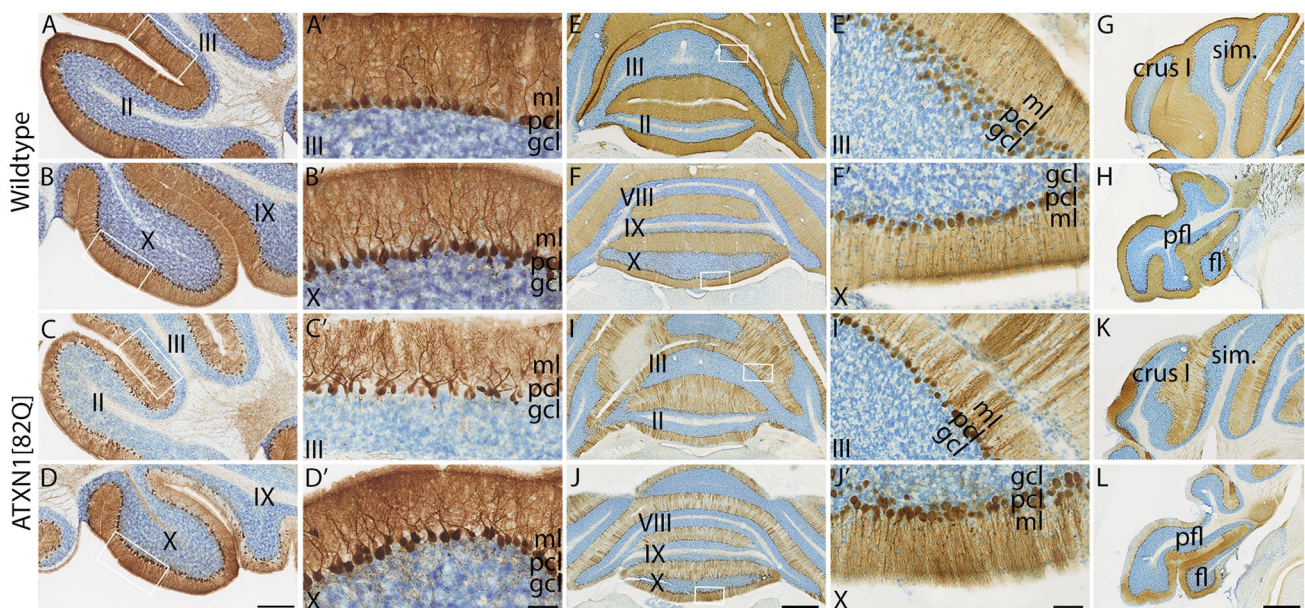

FIGURE 1   Purkinje cell degeneration is spared in a region-specific manner in 12-week ATXN1[82Q] mice. Purkinje cells in wild-type littermates show consistent morphology and calbindin labeling throughout the cerebellar cortex (A, B, A′, B′, E, F, E′, F′, G, H). Purkinje cells in ATXN1[82Q] mice exhibit severe degeneration in lobules II and III (C, C′, I, I′) as compared with lobule X (D, D′, J, J′), crus I (K), and the floccular complex (L). Scale bars: A–D = 250 μm, A′–D′ = 50 μm, E–L = 500 μm, E′–L′ = 50 μm. fl, flocculus; gl, granular layer; ml, molecular layer; pcl, Purkinje cell layer; pfl, paraflocculus; sim., lobulus simplex
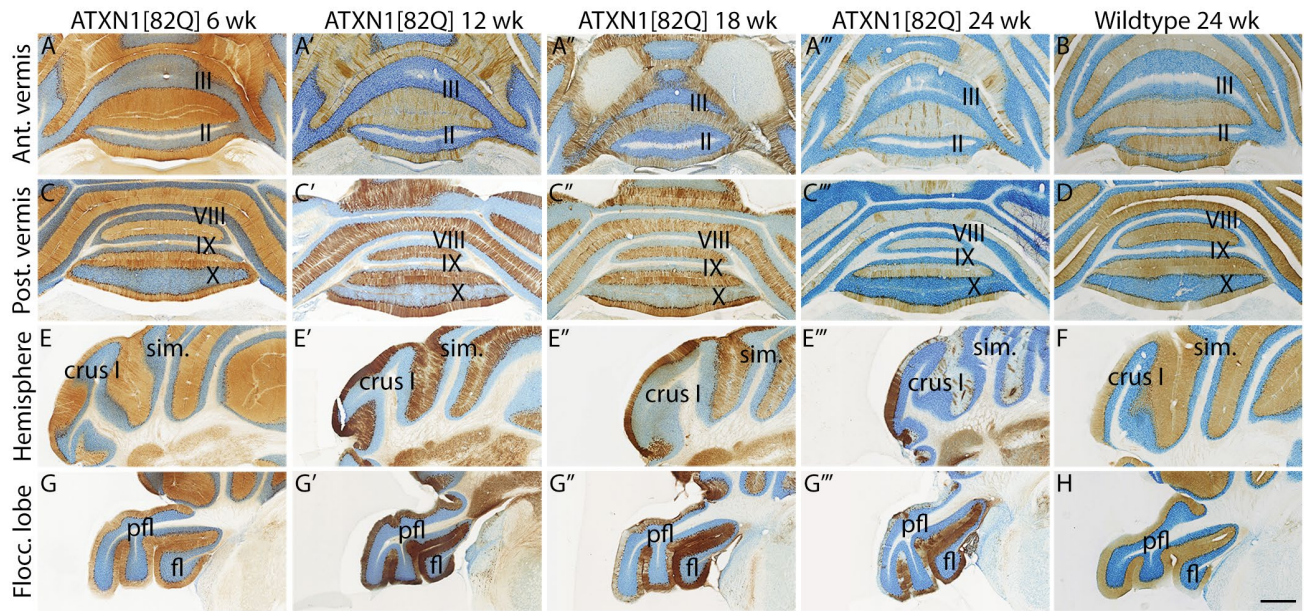
FIGURE 2 Purkinje cell degeneration is progressive in non-spared regions of the cerebellar cortex in ATXN1[82Q] mice. Spared regions remain spared at all ages. Regions that feature spared Purkinje cell morphology are highlighted and apparent with consistent calbindin staining. The anterior vermis (Ant. vermis) features the most severely atrophied Purkinje cells as compared with wild-type littermates (A–A‴, B). The posterior vermis (Post. Vermis) also features severe atrophy with the exception of lobule X (C–C‴, D). Other preferentially spared regions are crus I in the hemisphere (E–E‴, F) and the flocculus/ventral paraflocculus (G–G‴, H). Scale bar = 500 μm. Ant., anterior; wk, week; fl, flocculus; Flocc., floccular; pfl, paraflocculus; Post., posterior; sim., lobulus simplex

We also compared AldoC expression with an additional marker of Purkinje cell pathology, i.e., nuclear inclusions that represent a mid-late hallmark in ATXN1[82Q] Purkinje cells (43). To label nuclear inclusions, we stained for p62/SQSTM1 (p62 hereafter), an autophagy adaptor protein that is present at high levels in many neuronal inclusions, including intranuclear inclusions of SCA1 patients (44). In ATXN1[82Q] mice at 12 weeks, we found expression of p62-positive intranuclear inclusions in all Purkinje cells with somatodendritic atrophy, including those in lobules and zones that would typically express AldoC (Figure 4). Spared AldoC-positive Purkinje cells instead do not express p62-positive intranuclear inclusions (Figure 4). Together, these data indicate that there is complex relationship between AldoC expression and preservation of Purkinje cells in ATXN1[82Q] mice. Although apparently the preserved Purkinje cells are AldoC-positive, many Purkinje cells which normally express AldoC show the same pathological changes as AldoC-negative Purkinje cells in conjunction with loss of AldoC expression.

3.3 | Regional variations in Purkinje cell degeneration are due to incomplete transgene expression and independent of AldoC expression

The above data indicate that AldoC expression is an unreliable predictor of sparing from toxicity in ATXN1[82Q] mice. An alternative possibility would be that preservation of a subset of Purkinje cells is linked to differential mutant protein expression. To test this, we compared transgenic ATXN1[82Q] expression between spared and affected Purkinje cells using a rabbit polyclonal anti-ATXN1 antibody (antibody 11750) that produces weak nuclear staining in wild-type Purkinje cells and very strong nuclear staining in Purkinje cells of ATXN1[82Q] mice derived from the B05 line (45,46). Indeed, we found that a substantial portion of Purkinje cells in the flocculus and the nodulus of ATXN1[82Q] mice show weak or no nuclear staining for ATXN1 (Figure 5), while all affected Purkinje cells, including those in the flocculonodular lobes, show intense ATXN1 immunoreactivity. ATXN1 immunostaining in Purkinje cells of ATXN1[82Q] mice is binary: either very high or at the same level of Purkinje cells in wild-type animals. Based on this analysis, we define Purkinje cells in ATXN1[82Q] mice as either transgene positive or transgene negative, although very low expression in negative cells, and subtle differences in expression in positive cells cannot be excluded. Systematic analysis of all cerebellar lobules shows that, in all instances, affected Purkinje cells show high levels of mutant protein expression, while all spared Purkinje cells are negative for the transgene (Figure 5).

Closer inspection of the flocculus and the nodulus indicates that despite relative preservation, many Purkinje cells do express the mutant protein
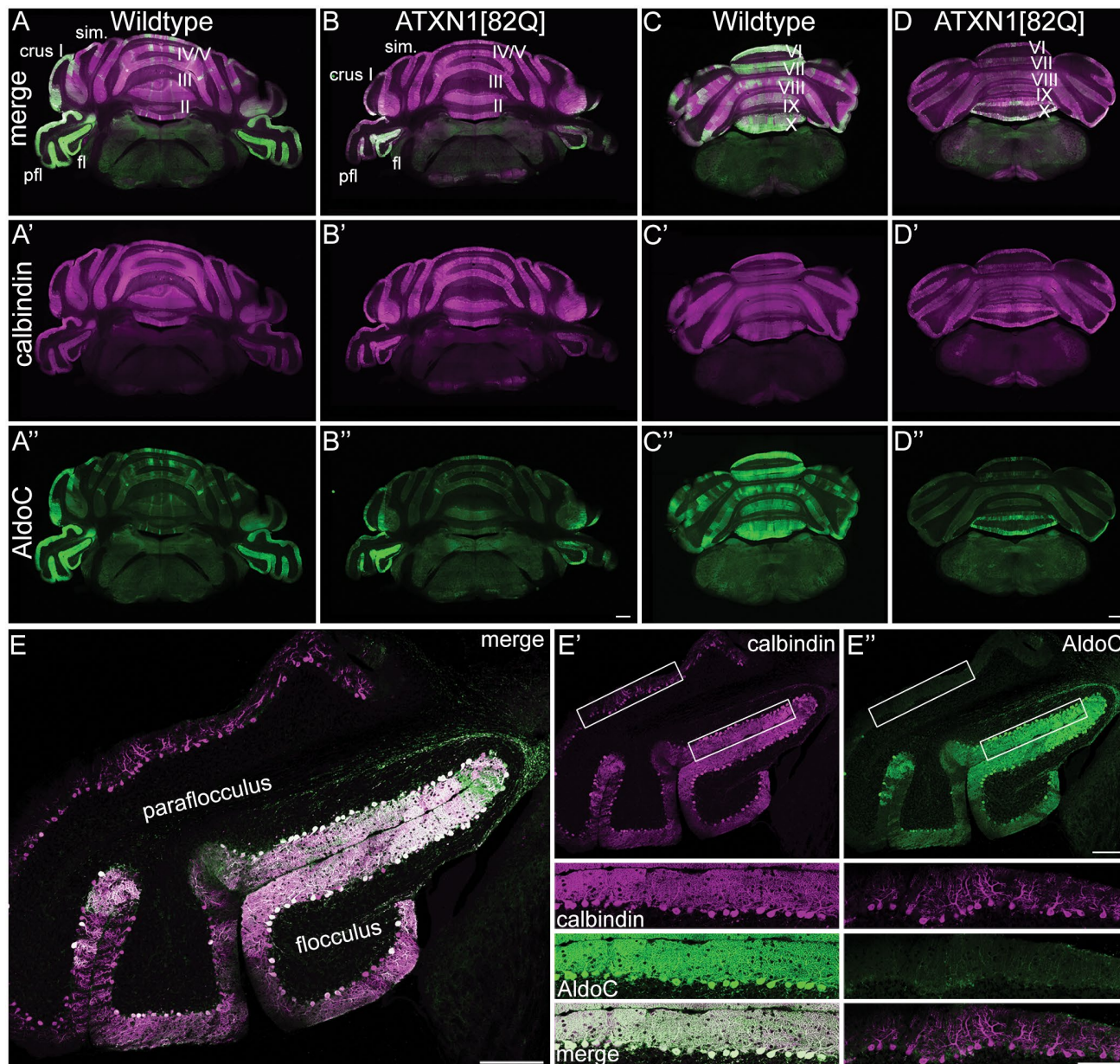
FIGURE 3 Lack of normal AldoC expression in Purkinje cells of 12-week ATXN1[82Q] mice is associated with degeneration. Spared Purkinje cells maintain their AldoC expression. The normal AldoC pattern (A–A″, C–C″) is disrupted in ATXN1[82Q] mice (B–B″, D–D″). Typically AldoC-positive regions, such as the dorsal paraflocculus (E, E′, E″), lose their AldoC identify and feature Purkinje cell atrophy. Scale bars = 500 μm (A–B″), 500 μm (C–D″), 200 μm (E), 200 μm (E′, E″), and 100 μm (E′ and E″ insets). fl, flocculus; pfl, paraflocculus; sim., lobulus simplex

and exhibit somatodendritic atrophy (Figure 5). In fact, somatodendritic atrophy to some extent was masked by calbindin staining of preserved Purkinje cells. Counting of the relative number of transgene-positive Purkinje cells revealed that ~45% of Purkinje cells express the transgene in the flocculus. For comparison, ~98% of the Purkinje cells express the transgene in lobules II and III of the vermis. These data indicate that the regional sparing of Purkinje cells in the ATXN1[82Q] mouse correlates with incomplete expression of the ATXN1 mutant protein.

3.4 | Specific motor behaviors are relatively spared in ATXN1[82Q] mice despite locomotor deficits

ATXN1[82Q] mice have previously been shown to display severe and progressive ataxia starting from 4 to 6 weeks of age (35,36). However, in view of the relative sparing of specific regions, we questioned whether this would allow for the relative preservation of specific cerebellar behaviors but not others. To this end, we performed four behavioral tests on ATXN1[82Q] mice between 6 and 24 weeks of age, consisting of a balance beam test
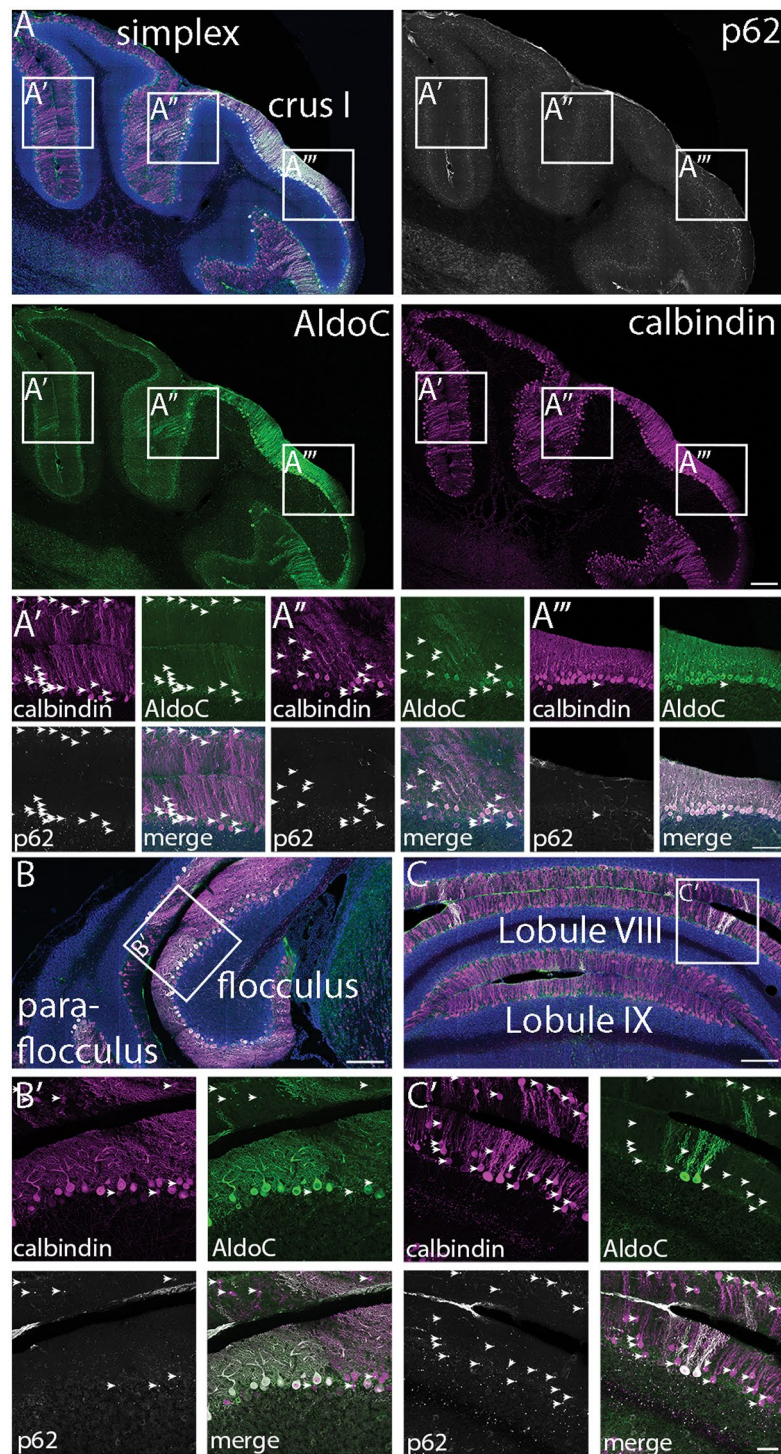
and locomotor test that require intact spinocerebellar regions, largely consisting of lobules I-V and lobule VIII of the vermis (47–49), and two tests that are linked to relatively preserved areas of ATXN1[82Q] mice: a licking test associated with crus I (50), and compensatory eye movements tests that require normal function of the flocculus (51).

The performance of the ATXN1[82Q] mice on the balance beam confirmed the development of progressive ataxia starting before 6 weeks of age (Figure 6A,B).

Their ability to walk along a 1 m wooden beam declined with age, with as few as 10% successful trials at 24 weeks of age. Deficits were already apparent at 7 weeks of age, as ATXN1[82Q] mice performed significantly worse than their wild-type littermates ($p < 0.001$, Fisher's exact tests after Benjamini–Hochberg correction for multiple comparisons; Figure 6B). Even if the ATXN1[82Q] mice were able to reach the other side of the beam, their travel times were longer than those of the wild-type littermates ($p < 0.01$, Mann–Whitney tests with
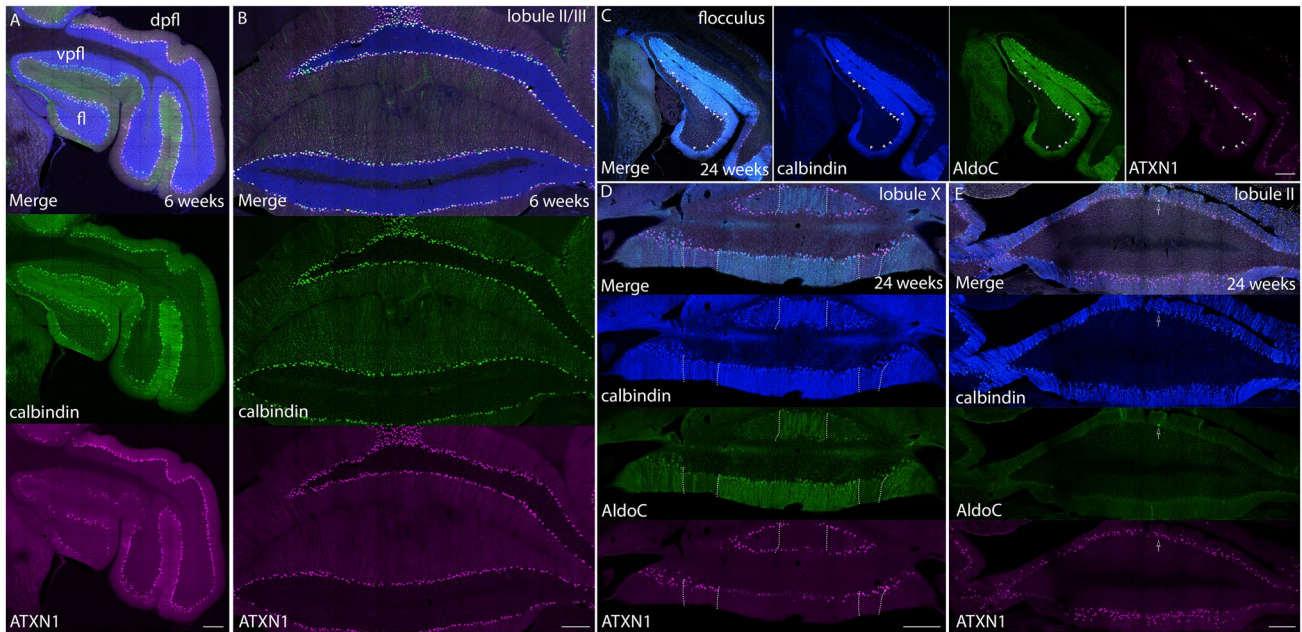
FIGURE 5 Purkinje cells in spared regions are less likely to express mutant ATXN1 in ATXN1[82Q] mice. The flocculus and ventral paraflocculus of ATXN1[82Q] contain fewer Purkinje cells expressing ATXN1 than the dorsal paraflocculus (A) or lobules II/III (B) at 6 weeks of age. This relationship also exists at 24 weeks and is associated with AldoC expression. In the flocculus, the subpopulation of Purkinje cells that expresses mutant ATXN1 does not express AldoC (arrowheads in C). This same relationship exists in the nodulus (lobule X) which has a higher likelihood of mutant ATXN1 expression in AldoC-negative bands (borders indicated with dotted lines in D). The vast majority of Purkinje cells in lobule II are atrophied and express mutant ATXN1, except for very rare healthy Purkinje cells which express AldoC (arrow in E). Scale bars = 200 μm. dpfl, dorsal paraflocculus; fl, flocculus; vpfl, ventral paraflocclus.

Benjamini–Hochberg correction for multiple comparisons; Figure 6B).

To further probe locomotor performance, we tested mice on the ErasmusLadder, a horizontal ladder with an alternating high/low pattern of rungs (Figure 6C). C57BL6/J mice show a strong preference for walking on the upper rungs, skipping one higher rung and avoiding lower rung touches, while cerebellar mutants show more lower rung steps and in addition show shorter steps (38,52). However, FVB/N wild-type mice of the current study exhibited more lower rung touches than C57BL6/J mice do and the number of lower rung touches was not significantly different between wild-type and ATXN1[82Q] mice ($p = 0.370$, $F_{1,19} = 0.844$, repeated measures ANOVA; Figure 6D). However, ATXN1[82Q] mice did make significantly fewer long steps ($p = 0.004$, $F_{1,19} = 10.689$, repeated measures ANOVA; Figure 6D), an effect that was already apparent from 12 weeks on ($p = 0.003$, $t_{18} = 3.482$, t-test, significant after Benjamini–Hochberg correction for multiple testing). The number of small steps was not significantly increased until 19 weeks ($p = 0.004$, $t_{18} = 3.361$, t-test, significant after Benjamini–Hochberg correction for multiple testing; Figure 6D). The smaller steps made by the mutant mice could not be explained by a decrease in body weight, as ATXN1[82Q] were on average even a bit heavier that their wild-type littermates, although this difference did not reach statistical significance (e.g.,

at 18 weeks: WT: median weight = 21.3 g (interquartile range = 9.4 g), ATXN1[82Q]: median = 26.9 g (interquartile range = 6.9 g), $p = 0.778$, $U = 50.5$, Mann–Whitney test). In conclusion, spinocerebellum-dependent behaviors including performance on the balance beam and the ErasmusLadder deteriorated progressively during the course of the disease.

In view of relative sparing of crus I, we performed a licking test that may require functional integrity of this lobule (50). Mice can lick at a sustained, high rate of up to 12 Hz (40), which can be affected by cerebellar damage (50,53). We measured the lick rates overnight in the home cages of ATXN1[82Q] mice and wild-type littermates (Figure 7). As we were interested in the licking speed, we focused on licking bouts with a maximal inter-lick interval of 150 ms (Figure 7A). There was no significant deficit in the licking frequency of the ATXN1[82Q] mice compared to their wild-type littermates at any age (WT: median frequency = 10.5 Hz (interquartile range = 0.4 Hz), ATXN1[82Q] = 10.1 Hz (0.4 Hz), $p = 0.136$, $U = 29.5$, Mann-Whitney test; Figure 7B). However, at 12 and 24 weeks, licking was slightly but significant more irregular in ATXN1[82Q] mice as compared to wild-type littermates (12 weeks: WT: CV2 = 0.095 (interquartile range = 0.008), ATXN1[82Q] = 0.106 (0.012), $p = 0.0208$, $U = 19$, Mann–Whitney test; 24 weeks: WT: CV2 = 0.091 (0.009), ATXN1[82Q] = 0.100 (0.012), $p = 0.0208$, $U = 19$, Mann–Whitney test; Figure 7B). Thus, we found only a
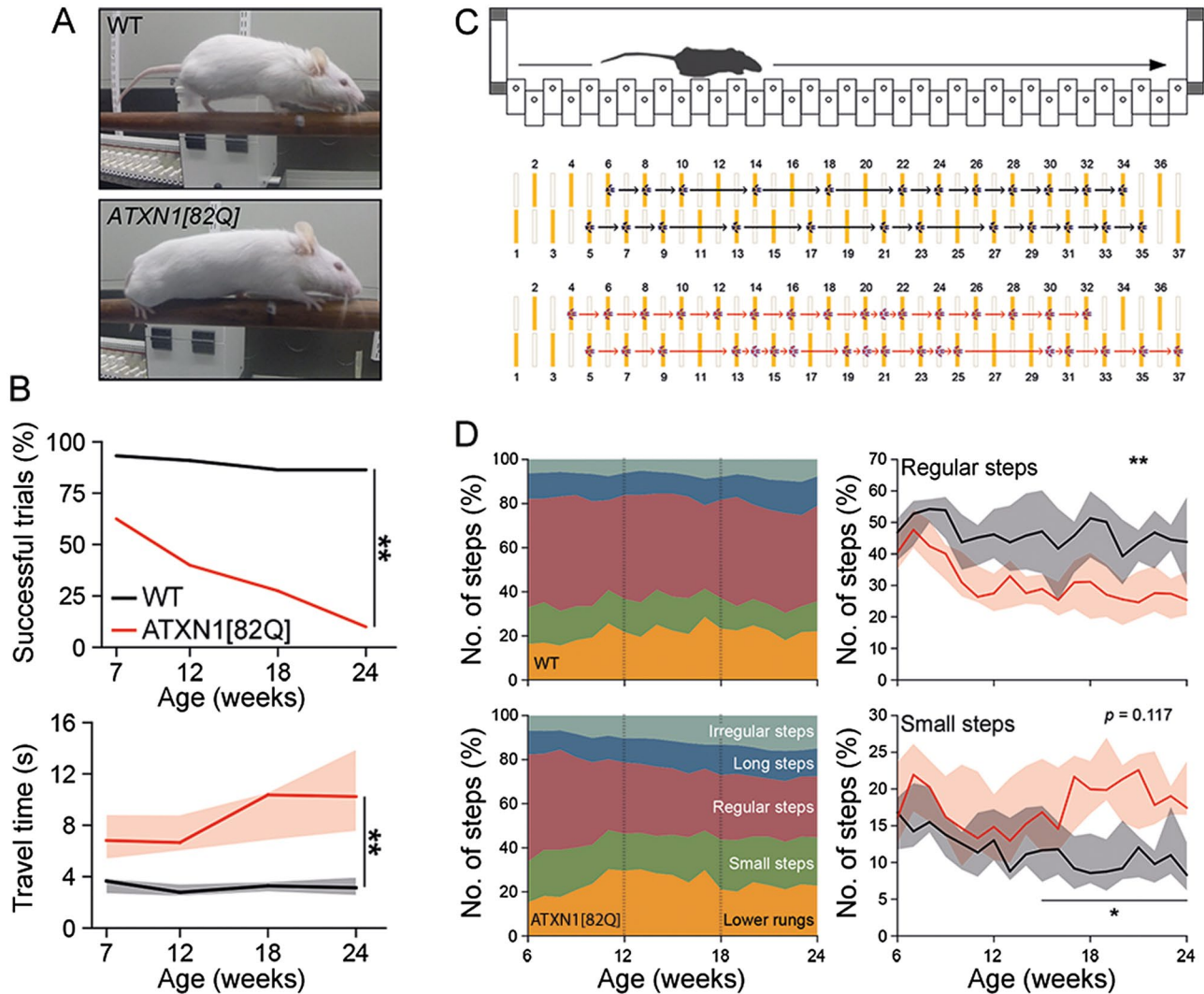
FIGURE 6 ATXN1[82Q] mice exhibit progressive deficit in motor coordination on both the balance beam and the ErasmusLadder. Example images of an ATXN1[82Q] mouse and wild-type littermate demonstrate typical posture on the balance beam (A). Compared to wild-type littermates, ATXN1[82Q] mice exhibit progressively decreasing percentage of successful balance beam trials and increased time to cross the beam (B). Representative examples of ErasmusLadder performance demonstrate the propensity for ATXN1[82Q] mice to make short steps as compared with wild-type littermates (C). Performance on the ErasmusLadder progressively changed over time (D). However, significant differences between groups were evident later in the disease progression than observed on the balance beam.

mild impact of the ATXN1[82Q] mutation on the ability to lick rhythmically at a high speed, but no impact on frequency.

Finally, we examined cerebellar behaviors associated with the flocculus. Compensatory eye movements include the optokinetic reflex (OKR), which is driven by movement of the visual field, and the vestibulo-ocular reflex (VOR), which is the response to head rotation or angular vestibular input, and require intact floccular lobules (54–59). Loss of floccular Purkinje cells results in a robust decrease in the gain of the OKR and VOR in the light (also referred to as visual or VVOR), both of which rely heavily on visual input. However, OKR and VVOR are largely intact in ATXN1[82Q] mice (Figure 8). There is no significant difference in OKR between ATXN1[82Q] mice and their control littermates

at 6 weeks, 12 weeks, or 18 weeks (Repeated Measures ANOVA: 6 weeks: $p = 0.215$, 12 weeks: $p = 0.187$; 18 weeks: $p = 0.142$). However, the VVOR gain is marginally, yet significantly, different at 6 weeks and 18 weeks, but not at 12 weeks (Repeated Measures ANOVA; 6 weeks: $p = 0.010$, 12 weeks: $p = 0.560$, 18 weeks: $p = 0.015$), there was no significant difference in phase of VVOR at any age (two-way ANOVA; 6 weeks: $p = 0.085$, 12 weeks: $p = 0.869$, 18 weeks: $p = 0.210$). There was a more prominent effect on VOR gain at the last time point tested (Repeated Measures ANOVA; 6 weeks: $p = 0.465$, 12 weeks: $p = 0.844$, 18 weeks: $p = 0.009$). Importantly, VOR gain increase adaptation, typically even more sensitive to cerebellar deficits than eye movement performance (55,56,60), was not impaired at any of the ages tested (Repeated Measures ANOVA; 6 weeks: $p = 0.116$,

FIGURE 7 Licking behavior is largely conserved in ATXN1[82Q] mice. Example licking traces for wild-type (WT) and ATXN1[82Q] mice demonstrate comparable behavior (A). There are no significant differences between groups in inter-lick interval at any age. However, a mild but significant difference was found in CV2 at 12 and 24 weeks ($p = 0.0208$) (B). Scale bar in A = 1 second.
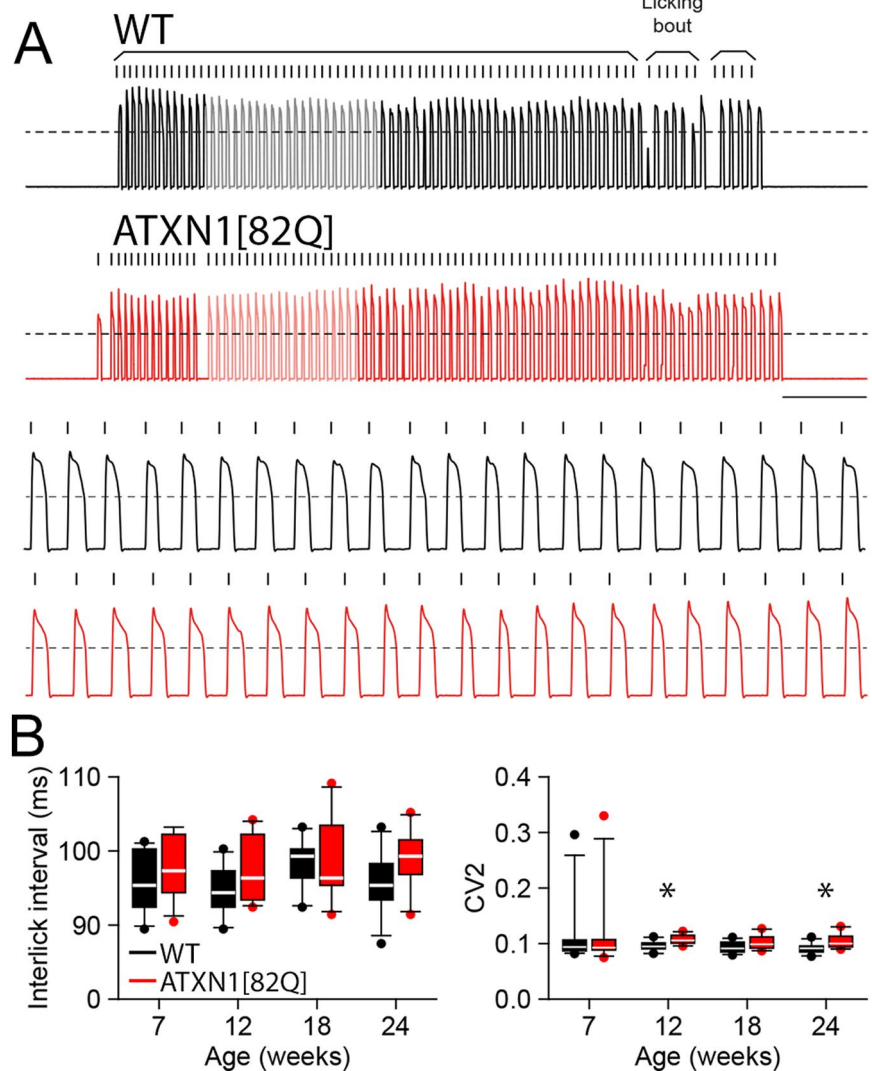
12 weeks: $p = 0.187$, 18 weeks: $p = 0.237$). In conclusion, unlike spinocerebellum-dependent behaviors, behaviors linked to crus I and the flocculus are relatively spared in ATXN1[82Q] mice.

4 | DISCUSSION

In this study, we aimed to further establish the causes and consequences of patterned Purkinje cell degeneration in the ATXN1[82Q] mouse model, a Purkinje cell degeneration mouse model designed to study disease mechanisms underlying SCA1. Based on previous studies of cerebellar patterned degeneration (16), our starting hypothesis was that AldoC-expressing Purkinje cells are relatively preserved, and that consequently cerebellar behaviors requiring AldoC-positive Purkinje cells are relatively intact, while behavior controlled by AldoC-negative Purkinje cells are severely affected. Our behavioral analyses are indeed consistent with this idea. There is preservation of compensatory eye movements and rhythmic licking, behaviors linked to the flocculonodular lobes

and crus I, respectively, which are also relatively preserved. In contrast, behaviors controlled by predominantly AldoC-negative, non-spared lobules are severely affected. However, our pathological analyses instead indicate that patterned Purkinje cell degeneration in ATXN1 mice does not correlate with differential AldoC expression in the same way that it does in other cerebellar degenerative models (16). Specifically, although we confirm that most preserved Purkinje cells are AldoC positive, this preservation is actually linked to absent (or much lower) transgene expression especially in the flocculus, nodulus, and crus I. Furthermore, we found that a large proportion of Purkinje cells that typically express AldoC, including those in caudal vermal lobules VII-IX and dorsal paraflocculus, exhibit the same pathology as AldoC-negative Purkinje cells in conjunction with complete loss of AldoC expression. This leads us to the conclusion that regional sparing in the ATXN1[82Q] mouse does not correlate with AldoC expression, but is based on an incomplete, region-specific transgene expression.

Our data place the ATXN1[82Q] mouse model in contrast to many rodent models of cerebellar disease
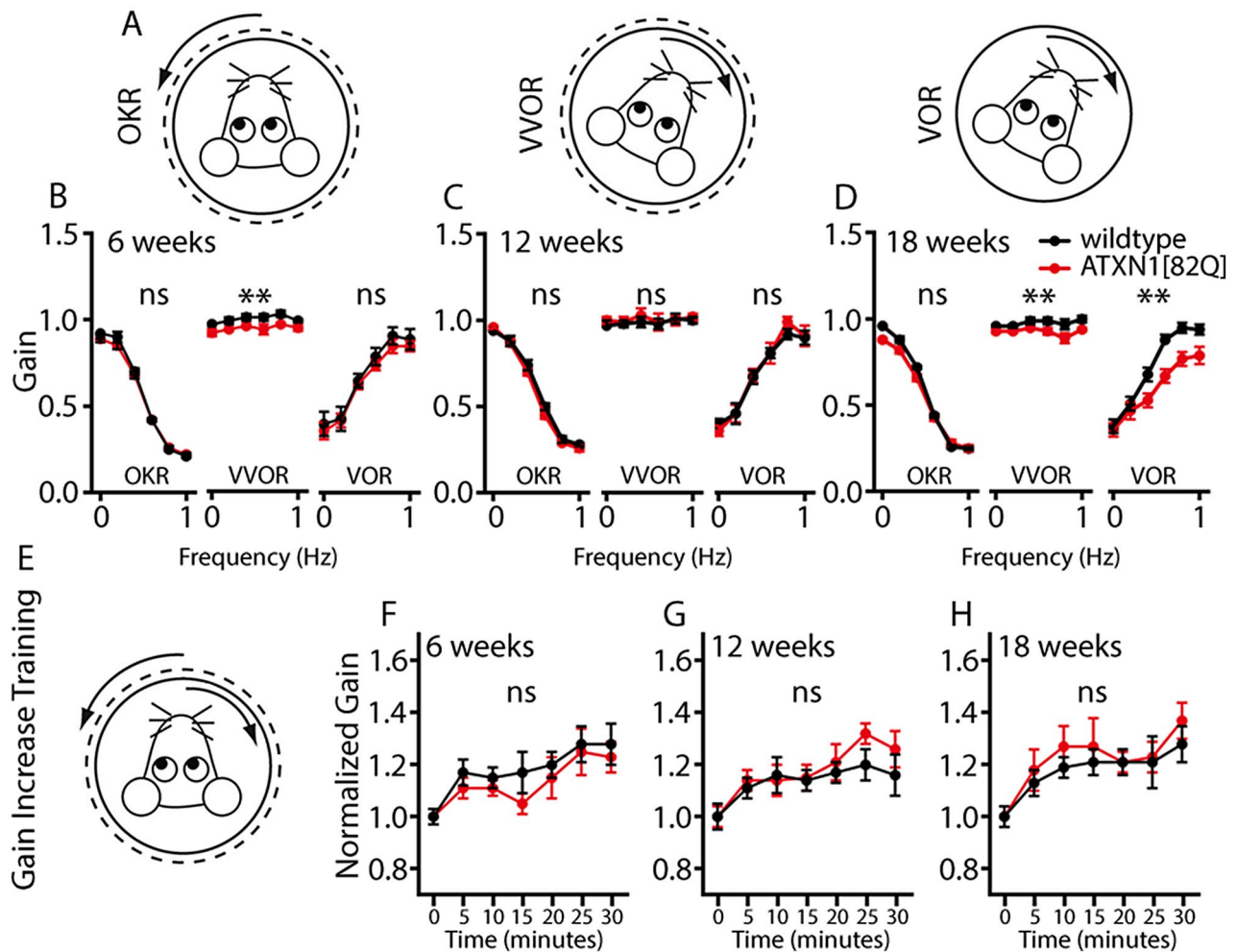
FIGURE 8 Compensatory eye movement behavior in ATXN1[82Q] mice is minimally affected at all ages tested. Three baseline eye movement behaviors were tested: the optokinetic reflex (OKR), visual vestibulo-ocular reflex (VVOR), and vestibule-ocular reflex (VOR) (A). At 6 weeks of age there are no significant differences between OKR and VOR, but the VVOR gain is marginally affected (B). There is no significant difference in any baseline eye movement behavior at 12 weeks of age (C). VVOR and VOR behaviors are significantly but mildly impaired at 18 weeks (D). In order to test cerebellar-dependent learning, mice underwent gain increase training (E) using out-of-phase visual and vestibular input, aimed at increasing the gain of the VOR. All values were normalized to the value before training (t = 0). There was no significant difference in gain increase training at any age tested (F, G, H). **indicates $p = 0.01$.

which exhibit cell death or degeneration preferentially in AldoC-negative Purkinje cells (16). Such a patterned degeneration is most clearly illustrated in leaner mouse that carries a mutation in a $Ca_V2.1$ subunit, and shows preservation of AldoC-positive Purkinje cells (61). Other cerebellar models of patterned degeneration with relative preservation of AldoC-positive Purkinje cells include other channelopathies (16,62,63), the lysosomal storage disorders Niemann-Pick disease type A/B and type C (16,64,65), and ischemia (33). The presence of similarly patterned atrophy/degeneration in these rodent models that lack any similarity in their pathogenic etiology suggests that genetic heterogeneity Purkinje cells (66,67) protect subpopulations of Purkinje cells to conditions affecting ionic and metabolic homeostasis. The absence of evidence favoring patterned degeneration in ATXN1[82Q] mice indicates that mutant ATXN1 unlike

other stressors may be damaging to all Purkinje cells independent of their neurochemical identity. ATXN1 is a DNA-binding protein and the polyQ expansion of ATXN1 induces massive transcriptional dysregulation in Purkinje cells, resulting in reduced expression of key physiological genes (68,69). Consistent with our data showing disruption of patterned AldoC expression in ATXN1[82Q] mice, it has been found that many genes with patterned expression in Purkinje cells like AldoC, PLCB3, KCTD12, and TRPC3 show severely reduced expression in cerebellar cortex of ATXN1[82Q] and other ATXN1 mice (68,69). These data raise the possibility that neurochemical heterogeneities between subpopulations of Purkinje cells may be lost in conditions impacting transcription as is suggested for SCA1 (68,69).

Mutant ATXN1 is selectively expressed in Purkinje cells in the ATXN1[82Q] mouse by the L7/Pcp2

promoter (35,70). Many versions of this promoter have been used in various mouse lines and modifications lead to a variety of patterns of expression in Purkinje cells (70–72). Based on this previous work, the long L7 promoter sequence used in the ATXN1[82Q] mouse was expected to result in expression in all Purkinje cells from an early postnatal age (35,70,72). However, our study demonstrates that this version of the promotor in this specific mouse line results in incomplete transgene expression in a small subset of lobules, putatively linked to transgenic site or other factors influencing the differential regulation of genes in Purkinje cells (72). The L7 promoter has been used in many other studies to drive gene expression specifically in Purkinje cells from an early postnatal age (58,70,73–78). While these studies have demonstrated aspects of the function of Purkinje cells, our findings highlight the need to verify expression or deletion of genes driven by a version of the L7 promoter before making conclusions that assume a complete expression of the genetic manipulation. There are many mouse lines using different versions of the L7 promoter (79) and each line may have a different expression pattern. However, the ATXN1[82Q] mouse model is especially vulnerable to incomplete transgene expression because the mutant gene is incorporated with the L7 promoter (35), as would be any mouse model using the same approach. Frequently, studies using the L7 promoter employ the Cre/Lox system in which genetic alterations are initiated by Cre-mediated recombination but driven by a different promoter such as Rosa (80,81). In that configuration, expression of Cre at any point in development will lead to a permanent expression or deletion of the targeted gene, whereas the ATXN1[82Q] mouse requires constant activity of the L7 promoter to drive the mutant gene. However, if Cre is never expressed due to incomplete expression driven by the L7 promoter, the genetic manipulation will be incomplete and will need to be assessed before conclusions can be made, depending on the aim of the study. The banded, incomplete pattern potentially driven by the L7 promoter is likely a result of the intrinsic organization and heterogeneity of Purkinje cells. As a result, whole regions may be spared which are related to specific cerebellar behaviors, further adding to the necessity to verify expression.

The spared regions in the ATXN1[82Q] mouse model include the flocculus and nodulus, which are involved primarily in eye movement (82). Additionally, crus I is spared, which receives somatosensory input from the orofacial region (83–85). In rodents, Purkinje cells in crus I are also involved in the motor control of orofacial behaviors, such as licking, whisking, and respiration (50,86,87). In humans, tongue movements seem to be more related to lobule VI (88), but crus I is activated during speech (89). The maintenance of behaviors related to these areas suggests that, even in the context of a severely degenerating neural population, selective sparing can result in differentiation in disease symptoms. Importantly, many Purkinje cells within the apparently spared regions express mutant ATXN1 that are not in fact spared, but it has been documented that the number of Purkinje cells necessary for motor behavior to remain normal is low (90). So any relative sparing can result in differentiation of disease symptoms.

Although in this model, regional sparing is caused by incomplete transgene expression, patterned degeneration is frequently observed in human cerebellar patients. Patterned degeneration in the cerebellum could potentially explain why some motor functions are affected earlier than others (15). SCAs are a group of neurodegenerative disorders that have a highly heterogeneous etiology as well as a broad spectrum of symptoms (9). Over 50 subtypes have been described, ranging from mutations in membrane channels to transcription factors (17,91,92). Of the most prevalent repeat expansion SCAs (SCA1, SCA2, SCA3, and SCA6), SCA1 has the fastest disease progress (93). At the end stage, there is widespread atrophy of, among other brain regions, the cerebellum, the pons, the brainstem, and the putamen, while the cerebral cortex is relatively spared (94). *Post mortem* studies demonstrate the partial loss of Purkinje cells in the cerebellum (95). There is some evidence for patterned degeneration and differential behavioral deficits in humans with cerebellar neurodegenerative disease. MRI results demonstrate unique degenerative signatures between different diseases (96). A voxel-based morphometry study found predominant loss of gray matter volume in the anterior vermis of SCA1 patients (97). Preferential anterior deficits have also been found in SCA3 and SCA6 (98). *Post mortem* tissue analysis has revealed marked differences in the degree of atrophy between cerebellar regions, at least in a number of spinocerebellar ataxias, including SCA1 (44,94,99–101). Indeed, SCA1 appears to sometimes lead to specific degeneration of the vermis and preservation of the flocculonodular lobes in human patients (101). Several analyses of oculomotor behavior in SCA patients have revealed a relative lack of deficits in SCA1 patients compared with other SCAs (102–104). Although a variety of eye movement defects are present in SCA1 patients, they appear to manifest at later stages in disease progression (105) and to a lesser extent than in other SCAs (106).

The modular organization of Purkinje cells based on molecular marker expression is conserved across species including humans (107,108). Our data show both that the expression pattern of mutated genes must be taken into account when analyzing differential susceptibility of Purkinje cells to specific disease but also that the sparing of specific regions of the cerebellar cortex will lead to sparing of specific behaviors even in the context of an otherwise unhealthy cerebellum. The maintenance of these behaviors indicates a mechanism for a functional reserve due to the anatomical

organization of the cerebellum. Understanding the modular organization of the cerebellum will be relevant to therapeutic approaches and should thus be further explored in this and other human cerebellar diseases.

CONFLICT OF INTEREST
None.

AUTHOR CONTRIBUTIONS
JJW and LWJB designed and performed experiments, analyzed the data, and wrote and revised the article. FB and CO designed and performed experiments. BWK, WHJJK, and CA performed experiments. CIDZ, DJ, and MS provided financial support and project supervision, and reviewed and revised the paper.

DATA AVAILABILITY STATEMENT
The data that support the findings of this study are available from the corresponding author upon reasonable request.

ORCID
Joshua J. White https://orcid.org/0000-0002-6218-623X
Laurens W. J. Bosman https://orcid.org/0000-0001-9497-0566
Francois G. C. Blot https://orcid.org/0000-0003-1472-9014
Catarina Osório https://orcid.org/0000-0002-5228-0599
Chris I. De Zeeuw https://orcid.org/0000-0001-5628-8187
Dick Jaarsma https://orcid.org/0000-0002-0519-2940
Martijn Schonewille https://orcid.org/0000-0002-2675-1393

REFERENCES
1. Fu H, Hardy J, Duff KE. Selective vulnerability in neurodegenerative diseases. Nat Neurosci. 2018;21:1350–8. https://doi.org/10.1038/s41593-018-0221-2
2. Saxena S, Caroni P. Selective neuronal vulnerability in neurodegenerative diseases: from stressor thresholds to degeneration. Neuron. 2011;71:35–48. https://doi.org/10.1016/j.neuron.2011.06.031
3. Comley L, Allodi I, Nichterwitz S, Nizzardo M, Simone C, Corti S, et al. Motor neurons with differential vulnerability to degeneration show distinct protein signatures in health and ALS. Neuroscience. 2015;291:216–29. http://dx.doi.org/10.1016/j.neuroscience.2015.02.013
4. Roselli F, Caroni P. From intrinsic firing properties to selective neuronal vulnerability in neurodegenerative diseases. Neuron. 2015;85:901–10. http://dx.doi.org/10.1016/j.neuron.2014.12.063
5. Mattsson N, Schott JM, Hardy J, Turner MR, Zetterberg H. Selective vulnerability in neurodegeneration: Insights from clinical variants of Alzheimer's disease. J Neurol Neurosurg Psychiatry. 2016;87:1000–4. https://doi.org/10.1136/jnnp-2015-311321
6. Brichta L, Greengard P. Molecular determinants of selective dopaminergic vulnerability in Parkinson's disease: an update. Front Neuroanat. 2014;8:1–16. https://doi.org/10.3389/fnana.2014.00152
7. Dawson TM, Dawson VL. Molecular pathways of neurodegeneration in Parkinson's disease. Science. 2003;302:819–22. https://doi.org/10.1126/science.1087753
8. Anheim M, Tranchant C, Koenig M. The autosomal recessive cerebellar ataxias. N Engl J Med. 2012;366:636–46. https://doi.org/10.1056/NEJMra1006610
9. Klockgether T, Mariotti C, Paulson HL. Spinocerebellar ataxia. Nat Rev Dis Prim. 2019;. https://doi.org/10.1016/B978-0-444-64189-2.00010-X
10. Rossi M, Anheim M, Durr A, Klein C, Koenig M, Synofzik M, et al. The genetic nomenclature of recessive cerebellar ataxias. Mov Disord. 2018;33:1056–76. https://doi.org/10.1002/mds.27415
11. Chopra R, Shakkottai VG. Translating cerebellar Purkinje neuron physiology to progress in dominantly inherited ataxia. Future Neurol. 2014;9:187–96. https://doi.org/10.2217/fnl.14.6
12. Cook AA, Fields E, Watt AJ. Losing the beat: contribution of Purkinje cell firing dysfunction to disease, and its reversal. Neuroscience. 2020. https://doi.org/10.1016/j.neuroscience.2020.06.008
13. Sen NE, Canet-Pons J, Halbach MV, Arsovic A, Pilatus U, Chae WH, et al. Generation of an Atxn2-CAG100 knock-in mouse reveals N-acetylaspartate production deficit due to early Nat8l dysregulation. Neurobiol Dis. 2019;132:104559. https://doi.org/10.1016/j.nbd.2019.104559
14. Zoghbi HY, Orr HT. Pathogenic mechanisms of a polyglutamine-mediated neurodegenerative disease, Spinocerebellar ataxia type 1. J Biol Chem. 2009;284:7425–9. https://doi.org/10.1074/jbc.R800041200
15. Luo L, Wang J, Lo RY, Figueroa KP, Pulst SM, Kuo P-H, et al. The initial symptom and motor progression in spinocerebellar ataxias. Physiol Behav. 2017;16:615–22. https://doi.org/10.1007/s12311-016-0836-3
16. Sarna JR, Hawkes R. Patterned Purkinje cell death in the cerebellum. Prog Neurobiol. 2003;70(6):473–507. https://doi.org/10.1016/S0301-0082(03)00114-X
17. Schorge S, van de Leemput J, Singleton A, Houlden H, Hardy J. Human ataxias: a genetic dissection of inositol triphosphate receptor (ITPR1)-dependent signaling. Trends Neurosci. 2010;33:211–9. https://doi.org/10.1016/j.tins.2010.02.005
18. Apps R, Hawkes R. Cerebellar cortical organization: a one-map hypothesis. Nat Rev Neurosci. 2009;10:670–81. https://doi.org/10.1038/nrn2698
19. Cerminara NL, Lang EJ, Sillitoe RV, Apps R. Redefining the cerebellar cortex as an assembly of non-uniform Purkinje cell microcircuits. Nat Rev Neurosci. 2015;16:79–93. https://doi.org/10.1038/nrn3886
20. Zhou H, Lin Z, Voges K, Ju C, Gao Z, Bosman LWJ, et al. Cerebellar modules operate at different frequencies. Elife. 2014;2014:1–3. https://doi.org/10.7554/eLife.02536
21. Apps R, Hawkes R, Aoki S, Bengtsson F, Brown AM, Chen G, et al. Cerebellar modules and their role as operational cerebellar processing units. Cerebellum. 2018;17(5):654–82. https://doi.org/10.1007/s12311-018-0952-3

22. Ahn AH, Dziennis S, Hawkes R, Herrup K. The cloning of zebrin II reveals its identity with aldolase C. Development. 1994;120:2081–90.

23. Brochu G, Maler L, Hawkes R. Zebrin II: a polypeptide antigen expressed selectively by Purkinje cells reveals compartments in rat and fish cerebellum. J Comp Neurol. 1990;291:538–52. https://doi.org/10.1002/cne.902910405

24. White JJ, Sillitoe RV. Development of the cerebellum: From gene expression patterns to circuit maps. Wiley Interdiscip Rev Dev Biol. 2013;2:149–64. https://doi.org/10.1002/wdev.65

25. Fujita H, Aoki H, Ajioka I, Yamazaki M, Abe M, Oh-Nishi A, et al. Detailed expression pattern of Aldolase C (Aldoc) in the cerebellum, retina and other areas of the CNS studied in Aldoc-Venus knock-in mice. PLoS One. 2014;9:22–7. https://doi.org/10.1371/journal.pone.0086679

26. Sugihara I. Crus I in the rodent cerebellum: its homology to Crus I and II in the primate cerebellum and its anatomical uniqueness among neighboring lobules. Cerebellum. 2018;17:49–55. https://doi.org/10.1007/s12311-017-0911-4

27. De Zeeuw CI, Ten Brinke MM. Motor learning and the cerebellum. Cold Spring Harb Perspect Biol. 2015;7:1–20. https://doi.org/10.1101/cshperspect.a021683

28. Horn KM, Pong M, Gibson AR. Functional relations of cerebellar modules of the cat. J Neurosci. 2010;30:9411–23. https://doi.org/10.1523/JNEUROSCI.0440-10.2010

29. Kakei S, Ishikawa T, Lee J, Honda T, Hoffman DS. Physiological and morphological principles underpinning recruitment of the cerebellar reserve. CNS Neurol Disord Drug Targets. 2018;17:184–92. https://doi.org/10.2174/1871527317666180315164429

30. Katoh A, Kitazawa H, Itohara S, Nagao S, Thompson RF. Dynamic characteristics and adaptability of mouse vestibulo-ocular and optokinetic response eye movements and the role of the flocculo-olivary system revealed by chemical lesions. Neurobiology. 1998;95:7705–10. https://doi.org/10.1073/pnas.95.13.7705

31. Xiao J, Cerminara NL, Kotsurovskyy Y, Aoki H, Burroughs A, Wise AK, et al. Systematic regional variations in Purkinje cell spiking patterns. PLoS One. 2014;9(8):e105633. https://doi.org/10.1371/journal.pone.0105633

32. Zhou H, Voges K, Lin Z, Ju C, Schonewille M. Differential Purkinje cell simple spike activity and pausing behavior related to cerebellar modules. J Neurophysiol. 2015;113:2524–36. https://doi.org/10.1152/jn.00925.2014

33. Welsh JP, Yuen G, Placantonakis DG, Vu TQ, Haiss F, O'Hearn E, et al. Why do Purkinje cells die so easily after global brain ischemia? Aldolase C, EAAT4, and the cerebellar contribution to posthypoxic myoclonus. Adv Neurol. 2002;89:331–59.

34. Dell'Orco JM, Wasserman AH, Chopra R, Ingram MAC, Hu Y-S, Singh V, et al. Neuronal atrophy early in degenerative ataxia is a compensatory mechanism to regulate membrane excitability. J Neurosci. 2015;35:11292–307. https://doi.org/10.1523/JNEUROSCI.1357-15.2015

35. Burright EN, Brent Clark H, Servadio A, Matilla T, Feddersen RM, Yunis WS, et al. SCA1 transgenic mice: a model for neurodegeneration caused by an expanded CAG trinucleotide repeat. Cell. 1995;82:937–48. https://doi.org/10.1016/0092-8674(95)90273-2

36. Clark H, Burright E, Yunis W, Larson S, Wilcox C, Hartman B, et al. Purkinje cell expression of a mutant allele of SCA1 in transgenic mice leads to disparate effects on motor behaviors, followed by a progressive cerebellar dysfunction and histological alterations. J Neurosci. 1997;17:7385–95. https://doi.org/10.1523/JNEUROSCI.17-19-07385.1997

37. Chopra R, Bushart DD, Cooper JP, Yellajoshyula D, Morrison LM, Huang H, et al. Altered Capicua expression drives regional Purkinje neuron vulnerability through ion channel gene dysregulation in spinocerebellar ataxia type 1. Hum Mol Genet. 2020;29:3249–65. https://doi.org/10.1093/hmg/ddaa212

38. Vinueza Veloz MF, Zhou K, Bosman LWJ, Potters JW, Negrello M, Seepers RM, et al. Cerebellar control of gait and interlimb coordination. Brain Struct Funct. 2015;220:3513–36. https://doi.org/10.1007/s00429-014-0870-1

39. Luong TN, Carlisle HJ, Southwell A, Patterson PH. Assessment of motor balance and coordination in mice using the balance beam. J Vis Exp. 2011;(49):5–7. https://doi.org/10.3791/2376

40. Rahmati N, Owens CB, Bosman LWJ, Spanke JK, Lindeman S, Gong W, et al. Cerebellar potentiation and learning a whisker-based object localization task with a time response window. J Neurosci. 2014;34:1949–62. https://doi.org/10.1523/JNEUROSCI.2966-13.2014

41. Holt GR, Softky WR, Koch C, Douglas RJ. Comparison of discharge variability in vitro and in vivo in cat visual cortex neurons. J Neurophysiol. 1996;75:1806–14. https://doi.org/10.1152/jn.1996.75.5.1806

42. Sugihara I, Quy PN. Identification of aldolase C compartments in the mouse cerebellar cortex by olivocerebellar labeling. J Comp Neurol. 2007;500:1076–92. https://doi.org/10.1002/cne.21219

43. Chuang C-S, Chang J-C, Soong B-W, Chuang S-F, Lin T-T, Cheng W-L, et al. Treadmill training increases the motor activity and neuron survival of the cerebellum in a mouse model of spinocerebellar ataxia type 1. Kaohsiung J Med Sci. 2019;35:679-85. https://doi.org/10.1002/kjm2.12106

44. Seidel K, Siswanto S, Brunt ERP, Den Dunnen W, Korf HW, Rüb U. Brain pathology of spinocerebellar ataxias. Acta Neuropathol. 2012;124:1–21. https://doi.org/10.1007/s00401-012-1000-x

45. Klement IA, Skinner PJ, Kaytor MD, Yi H, Hersch SM, Clark HB, et al. Ataxin-1 nuclear localization and aggregation: role in polyglutarnine- induced disease in SCA1 transgenic mice. Cell. 1998;95:41–53. https://doi.org/10.1016/s0092-8674(00)81781-x

46. Zu T, Duvick LA, Kaytor MD, Berlinger MS, Zoghbi HY, Clark HB, et al. Recovery from polyglutamine-induced neurodegeneration in conditional SCA1 transgenic mice. J Neurosci. 2004;24:8853–61. https://doi.org/10.1523/JNEUROSCI.2978-04.2004

47. Lackey EP, Sillitoe RV. Eph/ephrin function contributes to the patterning of spinocerebellar mossy fibers into parasagittal zones. Front Syst Neurosci. 2020;14:1–15. https://doi.org/10.3389/fnsys.2020.00007

48. Luo Y, Patel RP, Sarpong GA, Sasamura K, Sugihara I. Single axonal morphology and termination to cerebellar aldolase C stripes characterize distinct spinocerebellar projection systems originating from the thoracic spinal cord in the mouse. J Comp Neurol. 2018;526:681–706. https://doi.org/10.1002/cne.24360

49. Matsushita M. Projections from the lowest lumbar and sacral-caudal segments to the cerebellar cortex in the rat: an anterograde tracing study. Neurosci Res. 2017;114:43–54. https://doi.org/10.1016/j.neures.2016.09.013

50. Bryant JL, Boughter JD, Gong S, Ledoux MS, Heck DH. Cerebellar cortical output encodes temporal aspects of rhythmic licking movements and is necessary for normal licking frequency. Eur J Neurosci. 2010;32:41–52. https://doi.org/10.1111/j.1460-9568.2010.07244.x

51. Baarsma EA, Collewijn H. Vestibulo-ocular and optokinetic reactions to rotation and their interaction in the rabbit. J Physiol. 1974;238:603–25. https://doi.org/10.1113/jphysiol.1974.sp010546

52. Vinueza Veloz MF, Buijsen RAM, Willemsen R, Cupido A, Bosman LWJ, Koekkoek SKE, et al. The effect of an mGluR5 inhibitor on procedural memory and avoidance discrimination impairments in Fmr1 KO mice. Genes Brain Behav. 2012;11:325–31. https://doi.org/10.1111/j.1601-183X.2011.00763.x

53. Gaffield MA, Christie JM. Movement rate is encoded and influenced by widespread, coherent activity of cerebellar

molecular layer interneurons. J Neurosci. 2017;37:4751–65. https://doi.org/10.1523/JNEUROSCI.0534-17.2017

54. Aiba A, Kano M, Chen C, Stanton ME, Fox GD, Herrup K, et al. Deficient cerebellar long-term depression and impaired motor learning in mGluR1 mutant mice. Cell. 1994;79:377–88. https://doi.org/10.1016/0092-8674(94)90205-4

55. Boyden ES, Katoh A, Pyle JL, Chatila TA, Tsien RW, Raymond JL. Selective engagement of plasticity mechanisms for motor memory storage. Neuron. 2006;51(6):823–34. https://doi.org/10.1016/j.neuron.2006.08.026

56. Bruinsma CF, Schonewille M, Gao Z, Aronica EMA, Judson MC, Philpot BD, et al. Dissociation of locomotor and cerebellar deficits in a murine Angelman syndrome model. J Clin Invest. 2015;125:4305–15. https://doi.org/10.1172/JCI83541

57. Peter S, Ten Brinke MM, Stedehouder J, Reinelt CM, Wu B, Zhou H, et al. Dysfunctional cerebellar Purkinje cells contribute to autism-like behaviour in Shank2-deficient mice. Nat Commun. 2016;7:12627. https://doi.org/10.1038/ncomms12627

58. Schonewille M, Belmeguenai A, Koekkoek SK, Houtman SH, Boele HJ, van Beugen BJ, et al. Purkinje cell-specific knockout of the protein phosphatase PP2B impairs potentiation and cerebellar motor learning. Neuron. 2010;67:618–28. https://doi.org/10.1016/j.neuron.2010.07.009

59. Wulff P, Schonewille M, Renzi M, Viltono L, Sassoè-Pognetto M, Badura A, et al. Synaptic inhibition of Purkinje cells mediates consolidation of vestibulo-cerebellar motor learning. Nat Neurosci. 2009;12:1042–9. https://doi.org/10.1038/nn.2348

60. Galliano E, Potters J-W, Elgersma Y, Wisden W, Kushner S, De Zeeuw CI, et al. Synaptic transmission and plasticity at inputs to murine cerebellar Purkinje cells are largely dispensable for standard nonmotor tasks. J Neurosci. 2013;33:12599–618. https://doi.org/10.1523/JNEUROSCI.1642-13.2013

61. Heckroth JA, Abbott LC. Purkinje cell loss from alternating sagittal zones in the cerebellum of leaner mutant mice. Brain Res. 1994;658:93–104. https://doi.org/10.1016/s0006-8993(09)90014-2

62. Sawada K, Azad AK, Sakata-Haga H, Lee NS, Jeong YG, Fukui Y. Striking pattern of Purkinje cell loss in cerebellum of an ataxic mutant mouse, tottering. Acta Neurobiol Exp (Wars). 2009;69:138–45.

63. Wassef M, Sotelo C, Cholley B, Brehier A, Thomasset M. Cerebellar mutations affecting the postnatal survival of Purkinje cells in the mouse disclose a longitudinal pattern of differentially sensitive cells. Dev Biol. 1987;124:379–89. https://doi.org/10.1016/0012-1606(87)90490-8

64. Marques ARA, Aten J, Ottenhoff R, Van Roomen CPAA, Moro DH, Claessen N, et al. Reducing GBA2 activity ameliorates neuropathology in niemann-pick type C mice. PLoS One. 2015;10:1–18. https://doi.org/10.1371/journal.pone.0135889

65. Sarna J, Miranda SRP, Schuchman EH, Hawkes R. Patterned cerebellar Purkinje cell death in a transgenic mouse model of Niemann Pick type A/B disease. Eur J Neurosci. 2001;13:1873–80. https://doi.org/10.1046/j.0953-816x.2001.01564.x

66. Chung S-H, Calafiore M, Plane JM, Pleasure DE, Deng W. Apoptosis inducing factor deficiency causes reduced mitofusion 1 expression and patterned Purkinje cell degeneration. Neurobiol Dis. 2011;41:445–57. https://doi.org/10.1016/j.nbd.2010.10.016

67. Martin KB, Williams IM, Cluzeau CV, Cougnoux A, Dale RK, Iben JR, et al. Identification of novel pathways associated with patterned cerebellar purkinje neuron degeneration in niemann-pick disease, type C1. Int J Mol Sci. 2020;21: https://doi.org/10.3390/ijms21010292

68. Ingram M, Wozniak EAL, Duvick L, Yang R, Bergmann P, Carson R, et al. Cerebellar transcriptome profiles of ATXN1 transgenic mice reveal SCA1 disease progression and protection pathways. Neuron. 2016;89:1194–207. https://doi.org/10.1016/j.neuron.2016.02.011

69. Lin X, Antalffy B, Kang D, Orr HT, Zoghbi HY. Polyglutamine expansion down-regulates specific neuronal genes before pathologic changes in SCA1. Nat Neurosci. 2000;3:157–63. https://doi.org/10.1038/72101

70. Oberdick J, Smeyne RJ, Mann JR, Zackson S, Morgan JI. A promoter that drives transgene expression in cerebellar Purkinje and retinal bipolar neurons. Science. 1990;248:223–6. https://doi.org/10.1126/science.2109351

71. Oberdick J, Schilling K, Smeyne RJ, Corbin JG, Bocchiaro C, Morgan JI. Control of segment-like patterns of gene expression in the mouse cerebellum. Neuron. 1993;10:1007–18. https://doi.org/10.1016/0896-6273(93)90050-2

72. Vandaele S, Nordquist DT, Feddersen RM, Tretjakoff I, Peterson AC, Orr HT. Purkinje cell protein-2 regulatory regions and transgene expression in cerebellar compartments. Genes Dev. 1991;5:1136–48. https://doi.org/10.1101/gad.5.7.1136

73. Guo C, Witter L, Rudolph S, Elliott HL, Ennis KA, Regehr WG. Purkinje cells directly inhibit granule cells in specialized regions of the cerebellar cortex. Neuron. 2016;91:1330–41. https://doi.org/10.1016/j.neuron.2016.08.011

74. Gutierrez-Castellanos N, Da Silva-Matos CM, Zhou K, Canto CB, Renner MC, Koene LMC, et al. Motor learning requires Purkinje cell synaptic potentiation through activation of AMPA-receptor subunit GluA3. Neuron. 2017;93:409–24. https://doi.org/10.1016/j.neuron.2016.11.046

75. Lee KH, Mathews PJ, Reeves AMB, Choe KY, Jami SA, Serrano RE, et al. Circuit mechanisms underlying motor memory formation in the cerebellum. Neuron. 2015;86:529–40. https://doi.org/10.1016/j.neuron.2015.03.010

76. Lewis PM, Gritli-Linde A, Smeyne R, Kottmann A, McMahon AP. Sonic hedgehog signaling is required for expansion of granule neuron precursors and patterning of the mouse cerebellum. Dev Biol. 2004;270:393–410. https://doi.org/10.1016/j.ydbio.2004.03.007

77. Oberdick J, Levinthal F, Levinthal C. A Purkinje cell differentiation marker shows a partial DNA sequence homology to the cellular sis/PDGF2 gene. Neuron. 1988;1:367–76. https://doi.org/10.1016/0896-6273(88)90186-9

78. White JJ, Arancillo M, Stay TL, George-Jones NA, Levy SL, Heck DH, et al. Cerebellar zonal patterning relies on Purkinje cell neurotransmission. J Neurosci. 2014;34:8231–45. https://doi.org/10.1523/JNEUROSCI.0122-14.2014

79. Słupocka A, Wiaderkiewicz J, Barski JJ. Genetic targeting in cerebellar Purkinje cells: an update. Cerebellum. 2017;16:191–202. https://doi.org/10.1007/s12311-016-0770-4

80. Nagy A. Cre recombinase: the universal reagent for genome tailoring. Genesis. 2000;26:99–109. https://doi.org/10.1002/(SICI)1526-968X(200002)26:2<99::AID-GENE1>3.0.CO;2-B

81. Sauer B. Inducible gene targeting in mice using the Cre/lox system. Methods. 1998;392:381–92. https://doi.org/10.1006/meth.1998.0593

82. Ito M. Cerebellar control of the vestibulo-ocular reflex - around the flocculus hypothesis. Annu Rev Neurosci. 1982;5:275–96. https://doi.org/10.1146/annurev.ne.05.030182.001423

83. Bosman LWJ, Koekkoek SKE, Shapiro J, Rijken BFM, Zandstra F, van der Ende B, et al. Encoding of whisker input by cerebellar Purkinje cells. J Physiol. 2010;588:3757–83. https://doi.org/10.1113/jphysiol.2010.195180

84. Logan K, Robertson LT. Somatosensory representation of the cerebellar climbing fiber system in the rat. Brain Res. 1986;372:290–300. https://doi.org/10.1016/0006-8993(86)91137-6

85. Shambes GM, Gibson JM, Welker W. Fractured somatotopy in granule cell tactile areas of rat cerebellar hemispheres revealed by micromapping. Brain Behav Evol. 1978;15:94–140. https://doi.org/10.1159/000123774

86. Romano V, de Propris L, Bosman LWJ, Warnaar P, Ten Brinke MM, Lindeman S, et al. Potentiation of cerebellar purkinje cells facilitates whisker reflex adaptation through increased simple spike activity. Elife. 2018;7:1–33. https://doi.org/10.7554/eLife.38852

87. Romano V, Reddington AL, Cazzanelli S, Mazza R, Ma Y, Strydis C, et al. Functional convergence of autonomic and sensorimotor processing in the lateral cerebellum. Cell Rep. 2020;32:107867. https://doi.org/10.1016/j.celrep.2020.107867

88. Guell X, DE Gabrieli J, Schmahmann JD. Triple representation of language, working memory, social and emotion processing in the cerebellum: convergent evidence from task and seed-based resting-state fMRI analyses in a single large cohort. NeuroImage. 2018;172:437–49. https://doi.org/10.1016/j.neuroimage.2018.01.082

89. Correia JM, Caballero-Gaudes C, Guediche S, Carreiras M. Phonatory and articulatory representations of speech production in cortical and subcortical fMRI responses. Sci Rep. 2020;10:1–14. https://doi.org/10.1038/s41598-020-61435-y

90. Martin LA, Goldowitz D, Mittleman G. The cerebellum and spatial ability: Dissection of motor and cognitive components with a mouse model system. Eur J Neurosci. 2003;18:2002–10. https://doi.org/10.1046/j.1460-9568.2003.02921.x

91. Becker EBE. From mice to men: TRPC3 in cerebellar ataxia. Cerebellum. 2017;16:877–9. https://doi.org/10.1007/s12311-015-0663-y

92. Sullivan R, Yau WY, O'Connor E, Houlden H. Spinocerebellar ataxia: an update. J Neurol. 2019;266:533–44. https://doi.org/10.1007/s00415-018-9076-4

93. Diallo A, Jacobi H, Cook A, Labrum R, Durr A, Brice A, et al. Survival in patients with spinocerebellar ataxia types 1, 2, 3, and 6 (EUROSCA): a longitudinal cohort study. Lancet Neurol. 2018;17:327–34. https://doi.org/10.1016/S1474-4422(18)30042-5

94. Reetz K, Costa AS, Mirzazade S, Lehmann A, Juzek A, Rakowicz M, et al. Genotype-specific patterns of atrophy progression are more sensitive than clinical decline in SCA1, SCA3 and SCA6. Brain. 2013;136:905–17. https://doi.org/10.1093/brain/aws369

95. Rüb U, Schöls L, Paulson H, Auburger G, Kermer P, Jen JC, et al. Clinical features, neurogenetics and neuropathology of the polyglutamine spinocerebellar ataxias type 1, 2, 3, 6 and 7. Prog Neurogibol. 2013;104:38–66. https://doi.org/10.1016/j.pneurobio.2013.01.001

96. Hernandez-Castillo CR, King M, Diedrichsen J, Fernandez-Ruiz J. Unique degeneration signatures in the cerebellar cortex for spinocerebellar ataxias 2, 3, and 7. NeuroImage Clin. 2018;20:931–8. https://doi.org/10.1016/j.nicl.2018.09.026

97. Ginestroni A, Della Nave R, Tessa C, Giannelli M, De Grandis D, Plasmati R, et al. Brain structural damage in spinocerebellar ataxia type 1: A VBM study. J Neurol. 2008;255:1153–8. https://doi.org/10.1007/s00415-008-0860-4

98. Nanri K, Koizumi K, Mitoma H, Taguchi T, Takeguchi M, Ishiko T, et al. Classification of cerebellar atrophy using voxel-based morphometry and SPECT with an easy Z-score imaging system. Intern Med. 2010;49:535–41. https://doi.org/10.2169/internalmedicine.49.2785

99. Jacobi H, Hauser TK, Giunti P, Globas C, Bauer P, Schmitz-Hübsch T, et al. Spinocerebellar ataxia types 1, 2, 3 and 6: the clinical spectrum of ataxia and morphometric brainstem and cerebellar findings. Cerebellum. 2012;11:155–66. https://doi.org/10.1007/s12311-011-0292-z

100. Jung BC, Choi SI, Du AX, Cuzzocreo JL, Ying HS, Landman BA, et al. MRI shows a region-specific pattern of atrophy in spinocerebellar ataxia type 2. Cerebellum. 2012;11:272–9. https://doi.org/10.1007/s12311-011-0308-8

101. Robitaille Y, Schut L, Kish SJ. Structural and immunocytochemical features of olivopontocerebellar atrophy caused by the spinocerebellar ataxia type 1 (SCA-1) mutation define a unique phenotype. Acta Neuropathol. 1995;90:572–81. https://doi.org/10.1007/BF00318569

102. Anderson TJ, MacAskill MR. Eye movements in patients with neurodegenerative disorders. Nat Rev Neurol. 2013;9:74–85. https://doi.org/10.1038/nrneurol.2012.273

103. Buttner N, Geschwind D, Jen JC, Perlman S, Pulst SM, Baloh RW. Oculomotor phenotypes in autosomal dominant ataxias. Arch Neurol. 1998;55:1353–7. https://doi.org/10.1001/archneur.55.10.1353

104. Kim JS, Kim JS, Youn J, Seo DW, Jeong Y, Kang JH, et al. Ocular motor characteristics of different subtypes of spinocerebellar ataxia: distinguishing features. Mov Disord. 2013;28:1271–7. https://doi.org/10.1002/mds.25464

105. Stephen CD, Schmahmann JD. Eye movement abnormalities are ubiquitous in the spinocerebellar ataxias. Cerebellum. 2019;18:1130–6. https://doi.org/10.1007/s12311-019-01044-2

106. Moscovich M, Okun MS, Favilla C, Figueroa KP, Pulst SM, Perlman S, et al. Clinical evaluation of eye movements in spinocerebellar ataxias: a prospective multicenter study. J Neuro-Ophthalmology. 2015;35:16–21. https://doi.org/10.1097/WNO.0000000000000167

107. Marzban H, Hawkes R. On the architecture of the posterior zone of the cerebellum. Cerebellum. 2011;10:422–34. https://doi.org/10.1007/s12311-010-0208-3

108. Sillitoe RV, Marzban H, Larouche M, Zahedi S, Affanni J, Hawkes R. Conservation of the architecture of the anterior lobe vermis of the cerebellum across mammalian species. Prog Brain Res. 2004;148:283–97. https://doi.org/10.1016/S0079-6123(04)48022-4